Dual Mode Operation of GEM-3 as TD/FD Sensor

SERDP Final Technical Report

Seed Project Number UXO/1358

Geophex, Ltd.
605 Mercury St.
Raleigh, NC 27603-2343

Co-Principal Investigators: I.J. Won and Bill SanFilipo

Other participants:

Mike Shipman
Haoping Huang

Rev 1
June 28, 2004

Report Documentation Page

Form Approved
OMB No. 0704-0188

1. REPORT DATE	2. REPORT TYPE	3. DATES COVERED
28 JUN 2004		**00-00-2004 to 00-00-2004**

4. TITLE AND SUBTITLE	5a. CONTRACT NUMBER
Dual Mode Operation of GEM-3 as TD/FD Sensor	5b. GRANT NUMBER
	5c. PROGRAM ELEMENT NUMBER
6. AUTHOR(S)	5d. PROJECT NUMBER
	5e. TASK NUMBER
	5f. WORK UNIT NUMBER
7. PERFORMING ORGANIZATION NAME(S) AND ADDRESS(ES) **Geophex Ltd,605 Mercury St,Raleigh,NC,27603-2343**	8. PERFORMING ORGANIZATION REPORT NUMBER
9. SPONSORING/MONITORING AGENCY NAME(S) AND ADDRESS(ES)	10. SPONSOR/MONITOR'S ACRONYM(S)
	11. SPONSOR/MONITOR'S REPORT NUMBER(S)

12. DISTRIBUTION/AVAILABILITY STATEMENT
Approved for public release; distribution unlimited

13. SUPPLEMENTARY NOTES

14. ABSTRACT

15. SUBJECT TERMS

16. SECURITY CLASSIFICATION OF:			17. LIMITATION OF ABSTRACT	18. NUMBER OF PAGES	19a. NAME OF RESPONSIBLE PERSON
a. REPORT	b. ABSTRACT	c. THIS PAGE			
unclassified	**unclassified**	**unclassified**	**Same as Report (SAR)**	**21**	

Table of Contents

Acronyms

UXO ..... Unexploded Ordnance
FD ..... Frequency Domain
EMIS ..... Electromagnetic Induction Spectroscopy
TD ..... Time Domain
Tx ..... Transmitter
Qsum ..... Quadrature Sum
DevSum ..... Deviation from background time-domain Sum

Figures

Tables

Dual Mode Operation of GEM-3 as TD/FD Sensor

SERDP Final Technical Report, April 15, 2004
Seed Project Number UXO/1358
Co-Principle Investigators: I.J. Won and Bill SanFilipo, Geophex, Ltd.

Executive Summary

Electromagnetic geophysical exploration tools come in two types, frequency domain and time domain. A frequency-domain system utilizes continuous sinusoidal signals at one or more discrete frequencies, and the measurement consists of amplitude and phase (or real/inphase and imaginary/quadrature) response at each frequency; a time domain system utilizes abrupt step or pulse signals, and the measurement consists of time-sampled transient responses.

Historically, each has shown to be effective, but each with various claims of advantages over the other. In principle, time domain and frequency domain should provide equivalent information and one type of response to a target could be derived from the other. Complete equivalence can be shown for the ideal systems having infinite bandwidth/time interval and sample rate, and no noise. For real systems, it is not obvious how equivalent they are – i.e., does a particular time-domain system provide some information not easily attained with a particular frequency-domain system and vice versa? Are there real advantages of each over the other?

Until recently, technology constraints precluded building a sensor that could operate in both modes as effectively as a mode-tailored system, so no one ever did. Frequency-domain systems usually employed tuned high-Q resonant circuits to efficiently concentrate energy at the desired discrete frequencies, changing frequencies required switching the tuning circuit, and each frequency was operated one at a time. Time-domain systems employed a charge/discharge circuit not readily operated in a continuous-wave mode.

With the evolution of digital electronics and efficient high-current switching circuits, computer controlled systems with wide current waveform and signal processing flexibility are feasible. The GEM systems are built on this technology, and the standard continuous frequency domain operation is essentially a software feature rather than a hardware constraint. The GEM-3 sensor consists of three concentric coils – the outer most is the primary transmitter coil, the inner most the receiver coil, and between there is a secondary "bucking" transmitter that opposes the primary transmitter so as to create a primary magnetic field "cavity" around the receiver coil, dramatically reducing dynamic range requirements. This unique primary-field bucking scheme allows time-domain data to be recorded even during the current charge/discharge intervals.

This seed project involved developing the time-domain operational mode of the GEM-3 via essentially a software modification, and to further enhance the GEM-3 capability, provide an operational mode that alternated, at 15 Hz, between the frequency domain and the time domain.

We also developed preliminary processing schemes for unexploded ordnance (UXO) detection and discrimination using the time-domain data. A map of the Geophex test bed containing

various sized buried metal pipes shows that the time-domain data works well as a detection mode using a simple sum of the time gates. As a first attempt to discriminate, we applied a simple least-squares matching algorithm to the decay curves, allowing a linear combination of the longitudinal and transverse target modes. The results are similar to the frequency-domain performance, although a few particular target/geometry combinations worked better for one than the other. We tried one simple method of combining the two data modes – a simple averaging of the misfits. Tabulated results for both UXO items included in the matching library and clutter items not in the library are presented.

We envision further development, particularly in data fusion with processing algorithms tailored at maximizing the benefit of each type of data. Improvements to the time-domain operation may include some hardware fine-tuning as well as optimizing existing parameters such as on/off times and time-gate window intervals.

Objective

A general perception is that the TD mode may have an edge in detecting deep UXO, while it may not contribute much in target identification. We believe that the combined FD-TD data from a single EMI sensor would provide challenging but exciting opportunities for new data interpretation schemes for UXO detection and discrimination. The objective of this seed project is to develop prototype capability for simultaneous operation of a GEM-3 in frequency domain and time domain, where we mean by "simultaneous" as rapid, transparent switching between the two modes. We demonstrate target detection and characterization using each mode in which data were collected with a single GEM-3 with modified software that switches between modes at a 15 Hz rate, collecting 10 frequencies in the 30 Hz to 48 kHz range over alternating 30 Hz base periods, and 37 time gates over a total decay window of 2.167 ms. The actual frequencies and time gates are programmable. Some simple preliminary algorithms for processing the TD data have been used to show proof-of-concept for this mode with a GEM-3 instrument built originally as an FD instrument, and we compare performance for the two modes.

Project Background

The GEM-3 continuous wave frequency domain (FD) electromagnetic induction (EMI) sensor has demonstrated capability in target discrimination and classification via identifying targets using their characteristic responses over a broad range of frequencies, a process we have termed electromagnetic induction spectroscopy (EMIS). Most other EMI sensors in use today for UXO clearance are time-domain (TD) systems in which a transient response is measured at a set of time gates after a steady transmitter current is shut off. Although it has not been shown that either an FD or a TD system has a fundamental advantage, a question arises as to whether fusion of both types of sensor could prove to provide more information than either by itself. In principle, an idealized FD response could be converted to a TD response and vice versa through Fourier transform operations, but in practice, limits on frequencies or time gates sampled preclude even approximate transforms.

Developing a sensor with the capability to perform both as a FD and as a TD sensor will open the possibility to exploit advantages that each type of sensor may have over the other. Although

many EMI sensors for geophysical applications utilize hardware that is tailored for the specific operational mode, a sensor that uses a flexible hardware design has the potential to perform in both modes with software. Since a GEM-3 sensor is all digital and broadband, it is a candidate for dual mode operation.

Hardware and Methods

Hardware for this project consisted of an existing 64 cm diameter GEM-3 sensor (Figure 1) with modified software to provide alternating time and frequency domain operation at 15 Hz each. Modified user interface software (hand-held computer based) provided means to set up and operate the sensor, and log data. We also developed prototype post-processing software to generate time-domain detection channel and target matching results.

Methods used included measuring calibration targets (ferrite rod) and a number of test targets consisting of sample UXO and metallic clutter items in standard frequency domain and dual modes, and compare standard frequency domain and dual mode performance.

Figure 1. Various GEM-3 sensor configurations include the hand-held 40 cm (left) and 64 cm (center), and cart-mounted 96 cm versions. The 64 cm coil was used for the dual-mode data presented in this project.

Results and Accomplishments

Dual Mode Capable GEM-3

A standard GEM-3 electronics console has been loaded with new software to control the dual mode operation of the sensor and record data for each. Also, a special version of WinceGEM software, the standard iPAC Windows CE-based GEM-3 user-interface software for downloading, logging, and displaying dual mode data was written. The raw time sampling following the current shutoff during a TD interval is 96 kHz as in the FD mode. Storing the raw samples would result in an excessive amount of data, so the GEM digital signal processor combines (integrates) multiple points over variable length time gates that progressively expand with delay time. The 37 specific time gates used are given in Table 1. The time gates are designed to provide high temporal resolution, especially at early times during rapid changes, and noise reduction via integration at late times when the signal is weak.

Gate #	1	2	3	4	5	6	7	8
Center time (μs)	5	16	26	36	47	57	68	78
Time interval (μs)	10	10	10	10	10	10	10	10
Gate #	9	10	11	12	13	14	15	16
Center time (μs)	89	99	115	135	156	177	214	245
Time interval (μs)	10	10	21	21	21	21	31	31
Gate #	17	18	19	20	21	22	23	24
Center time (μs)	276	318	359	401	453	505	557	620
Time interval (μs)	31	31	31	31	52	52	52	73
Gate #	25	26	27	28	29	30	31	32
Center time (μs)	693	766	849	943	1047	1161	1286	1422
Time interval (μs)	73	73	94	94	115	115	135	135
Gate #	33	34	35	36	37			
Center time (μs)	1557	1703	1859	2016	2172			
Time interval (μs)	135	156	156	156	156			

Table 1. TD mode time gate center time (from current shutoff) and gate time intervals, formed by averaging raw 96 kHz samples. The first ten gates are single samples, and the last four gates are 15 samples each.

During a single 30 Hz TD interval, multiple step response transients are recorded, the number and duration programmable, with each transient in the first 30 Hz half interval (i.e. one 60 Hz interval) associated with a transient in the second 30 Hz half interval (i.e. delayed by 1/60th second) having opposite current polarity. Stacking (subtracting to account for current reversal) these pairs ensures suppression of ambient 60 Hz noise. Multiple pairs recorded during the 30 Hz interval can then be stacked for further noise rejection, the number limited only by the on/off time recording desired for each transient measured. The dual-mode operation alternates between these 30 Hz TD intervals and the standard 30 Hz FD intervals during which a hybrid current waveform containing a continuous multi-frequency signal (Figure 2).

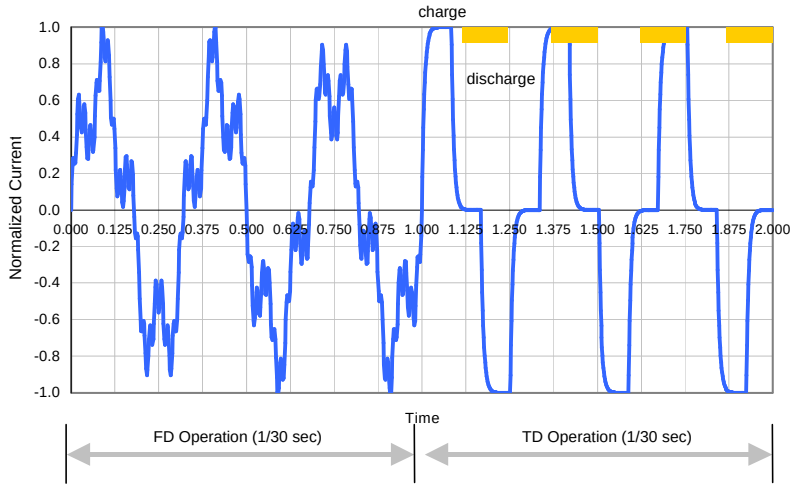

Figure 2. An example FD-TD waveform that can be used by the GEM-3

The time gate signal voltages are normalized by the reference channel voltage integrated over the entire measurement window; the earliest time includes residual transmitter current and thus the reference provides a current amplitude normalization as in the FD mode.

A simple detection channel consists of the sum of the time gate transient measurements over a programmable window (i.e. an integrated response), and with background subtracted, referred to as DevSum. This parameter has been included in the special version of our iPAC software as a real-time target detection option.

Time Domain Functionality

In order to verify the new TD capability of the GEM-3 and better understand its performance characteristics, we measured the TD response of two spheres with known properties (based on FD measurements) and compared them with models.

The models were generated as follows: First, the current waveform was modeled based on the voltage, transmitter (Tx) coil inductance and resistance and current limit (current turn-on follows an L-R circuit until the maximum allowed current is attained, and then held for the duration of the specified on time), and the measured turn-off ramp (the current off ramp is determined by the open loop distributed capacitance of the Tx coil forming an R-C circuit, and was measured by the reference coil, which indicated a nearly constant voltage for 42 μs corresponding to a linear current-off ramp), and the specified on-time, off-time. The primary induction waveform was computed as the analytic time derivative of the current waveform, which was then transformed to the frequency domain using an FFT. Next, the FD sphere response over a broad range of frequencies was computed using an analytical algorithm, which was then multiplied by the primary induction FD spectrum. Since the GEM-3 system has a transfer function that is accounted for in the FD mode with calibration factors for each frequency, the ideal FD response is divided by the calibration factors to incorporate the GEM-3 transfer function. Finally, the FD model is transformed into the time domain using an inverse FFT.

In Figures 3 and 4 we compare the predicted to measured TD response to a stainless-steel ball and a steel shot put respectively. The first 42 μs are during the current ramp-off, indicated by the strong positive response while eddy currents build up in the target.

The difference in character between the two targets corresponds to the (nearly) non-ferrous stainless steel versus the ferrous steel; the ferrous target has a sign-flip during the current ramp followed by a strong positive peak, and the late-time is not a single-mode exponential, while the non-ferrous sign-flip occurs when the current ramp ends and the eddy currents immediately start to decay, and the late-time is very nearly a single-mode exponential decay.

The measured results agrees reasonably well with the model (the shot put FD measurements do not fit the FD model perfectly either), except for the amplitude of the stainless steel ball during the current ramp (corresponding to eddy current buildup in the target).

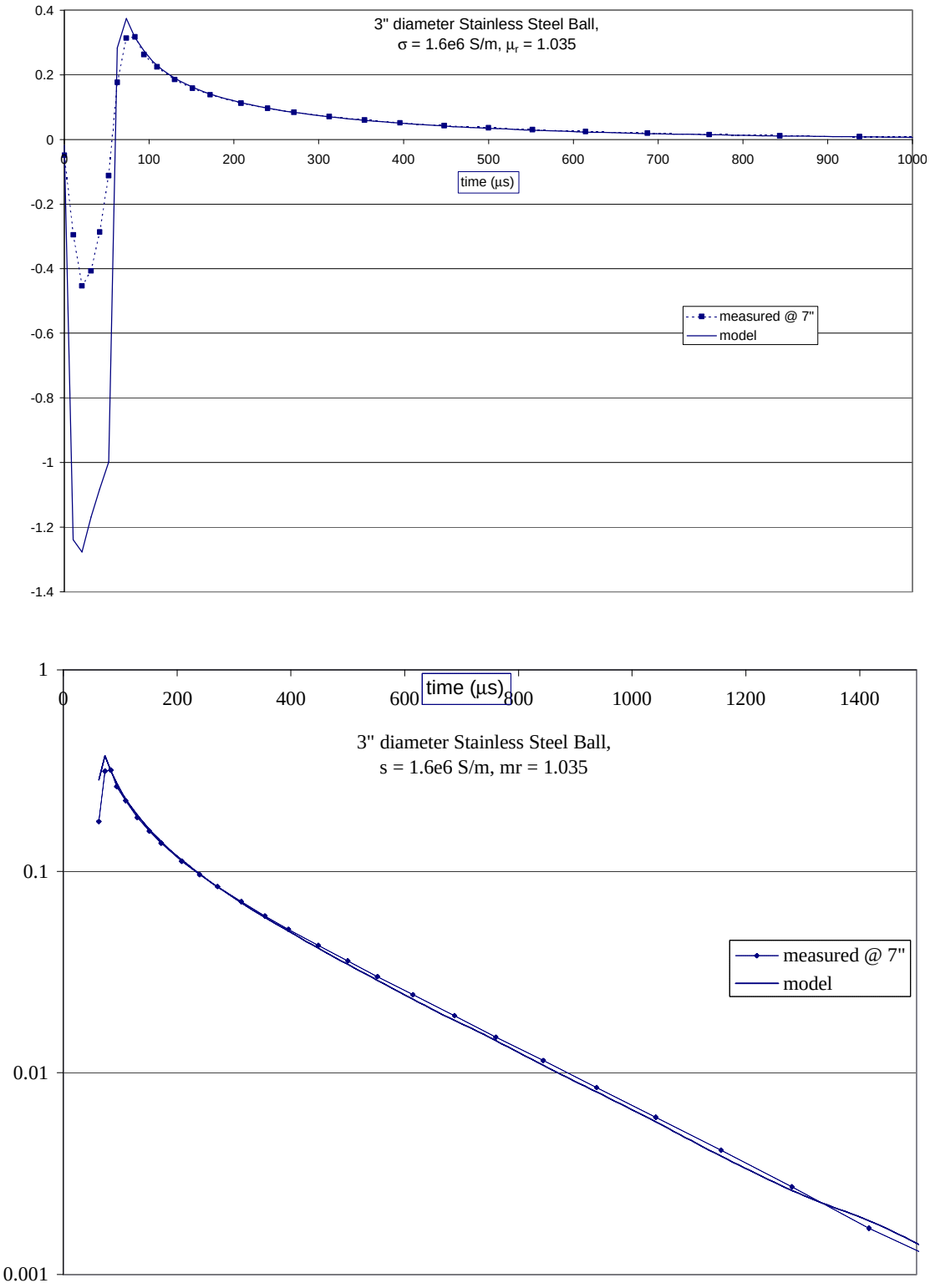

Figure 3. The GEM-3 TD response to a three-inch diameter stainless-steel ball, showing the first millisecond including the initial 42 μs current ramp-off interval (top), and the log scale from the end of the ramp to 1.6 ms.

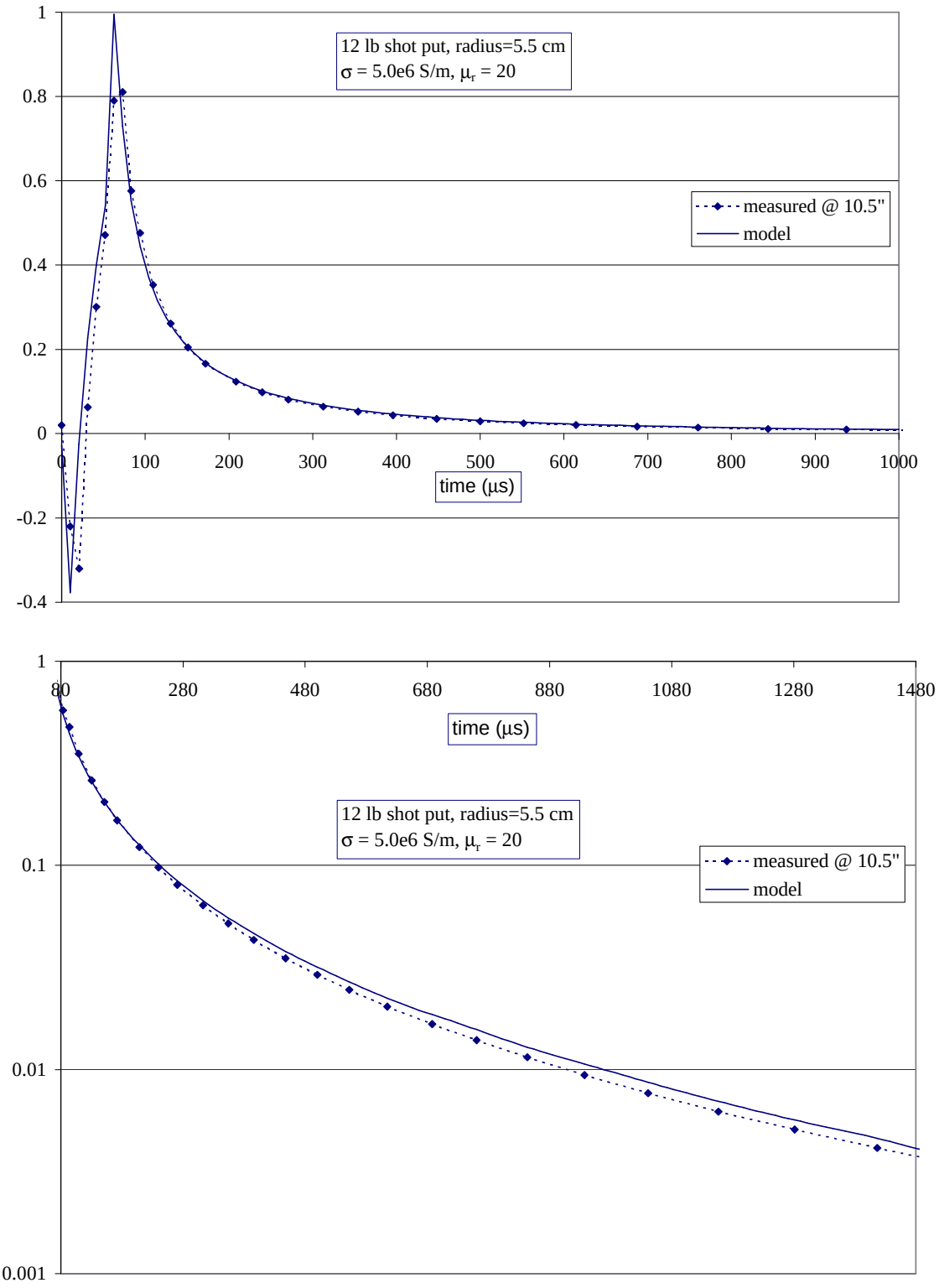

Figure 4. The GEM-3 TD response to a 12 lb shot put, showing the first millisecond including the initial 42 μs current ramp-off interval (top), and the log scale from the end of the ramp to 1.48 ms.

Experiments

Survey - Detection

Our first experiment was a dual-mode survey over our backyard test site containing buried pipes with a 64 cm diameter sensor mounted on a wheeled cart. For comparison, we repeated the survey with the same hardware, but using standard (continuous) frequency domain only firmware. We compared the FD detection channel (sum of all frequency quadrature components, termed QSum) from the dual mode data with the TD channel (DevSum), and with the FD channel from the standard FD configuration. Color contour maps for these three data sets are presented in Figure 5, including a site map showing the targets.

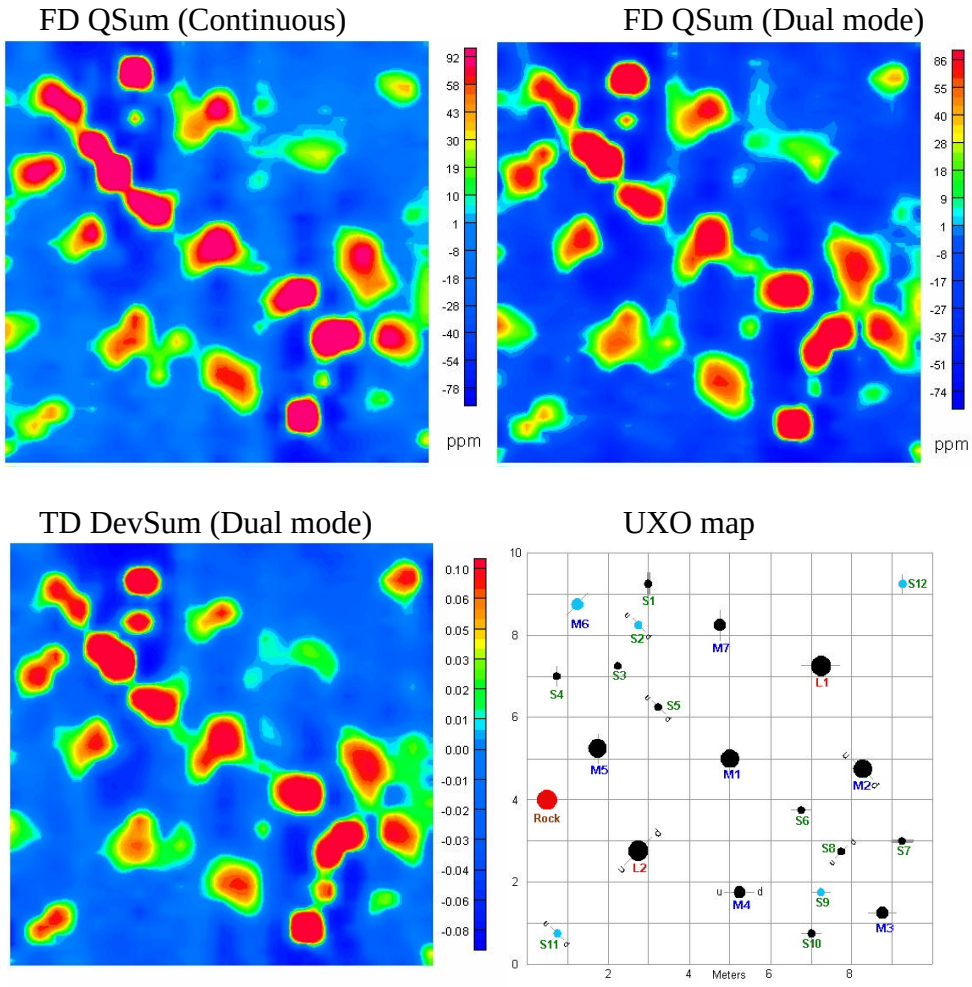

Figure 5. Comparison of target detection channel maps from data recorded over the Geophex buried-pipe test bed; two surveys were performed, one in continuous (standard) FD mode providing data for the upper-left map, and one in dual mode providing data for both the upper right and lower left maps. The site map (lower right) shows the location of buried targets, blue signifying non-ferrous, "S" signifying small, "M" medium, and "L" large (the larger targets are buried deeper).

All three maps show excellent detection of the buried pipes with similar quality. The small non-ferrous targets (S2, S9, S11, S12) appear somewhat more pronounced in the TD map. Note that the continuous FD utilizes 30 Hz sampling and thus benefits from double the data as in the other two maps.

Target Characterization

Dual-mode data were collected for a number of UXO items (20mm – 80mm range, Figure 6) and clutter items (Figure 7) on a test stand using the same sensor as the backyard survey. A library for the UXO items was made with the target oriented longitudinal and transverse with respect to the GEM coil axis for each mode. For reasons not yet understood, the non-ferrous UXO items (40mm) produced responses that were fundamentally different (sign inversion) at five-inch and nine-inch heights (Figure 8), although the FD spectral responses differed by a scale factor as expected for a dipole type response. The ferrous objects did not exhibit this behavior, and also did not change sign during the decay as in the aluminum target responses (Figure 9). The zero crossing during the early decay occurred consistently for the non-ferrous clutter but not the ferrous clutter as well as for the UXO items.

The following UXO test targets were used:

UXO70 — 20mm projectile	(ferrous)
UXO12 — 40mm projectile	(non-ferrous)
UXO92 — 40mm projectile with casing	(non-ferrous except for thin-walled casing)
UXO13 — 37mm projectile	(ferrous)
UXO5 — 60mm mortar with fins	(ferrous)
UXO9 — 80mm mortar with fins	(ferrous)

Figure 6. UXO test items used in the FD and TD target classification tests.

In addition, the following 16 clutter items were measured: penny, nickel, dime, quarter, steel pipe (1? ”OD, 4”L), copper pipe (1”OD, 6”L), aluminum pipe (1”OD, 6”L), short screwdriver (3½”L), nail (10D, 3”L), nut (7/8 inch), bolt (3¼ inch), crushed Coke can, large paper clip, brass fitting (1½ inch), twisted coat hanger, brass disk (2”D, 1”H), bookend, paint can lid (bent), and a metal UXO fragment.

Figure 7. Clutter test items used in the FD and TD target classification tests.

We also collected standard continuous FD data, which were used for the TD comparison presented here. Subsequent to the library generation, we collected TD and FD data for the targets at multiple heights, oriented at about 45º. These data were processed with our matching algorithms (simple linear combination of longitudinal and transverse library responses), and the fitting error used to classify as probable clutter. The TD fitting algorithm was a simple adaptation of the FD algorithm using different time gates analogous to different frequencies. No weighting as a function of delay time was utilized, and the squared-error sum was normalized by the squared amplitude sum over the time gates used (similar to the FD normalized squared-error sum).

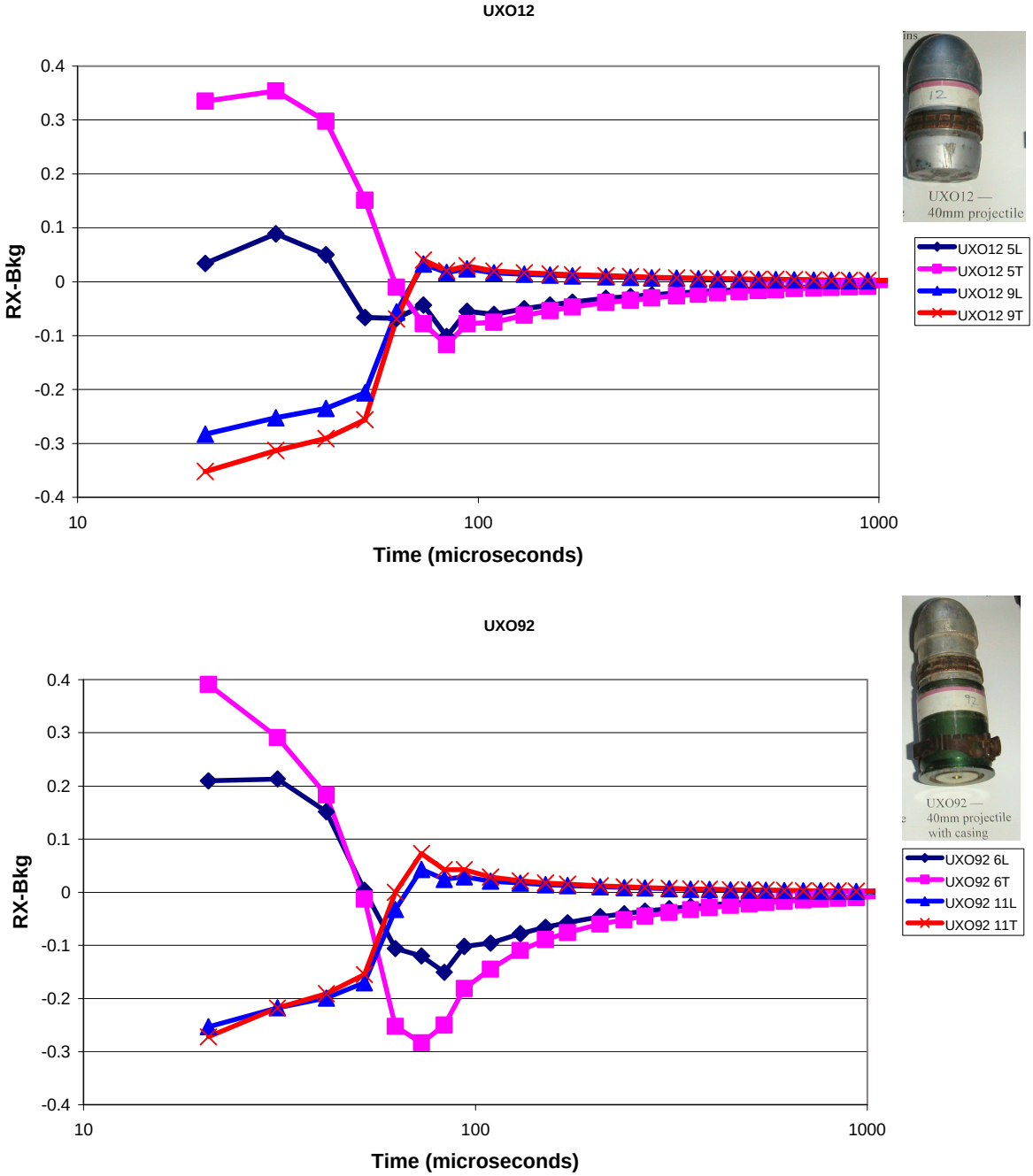

Figure 8. Comparison of the response at 5 and 9 inches height of the aluminum 40mm UXO item #12 (top), and at 6 and 11 inches height of the aluminum 40mm UXO item #92 with steel casing (bottom), showing sign inversion between the two heights. The "T" refers to transverse mode (target oriented long axis perpendicular to sensor coil axis), and "L" the longitudinal mode (target oriented long axis parallel to sensor coil axis). Note the logarithmic time scale, which shows early time behavior, including zero crossing during the decay.

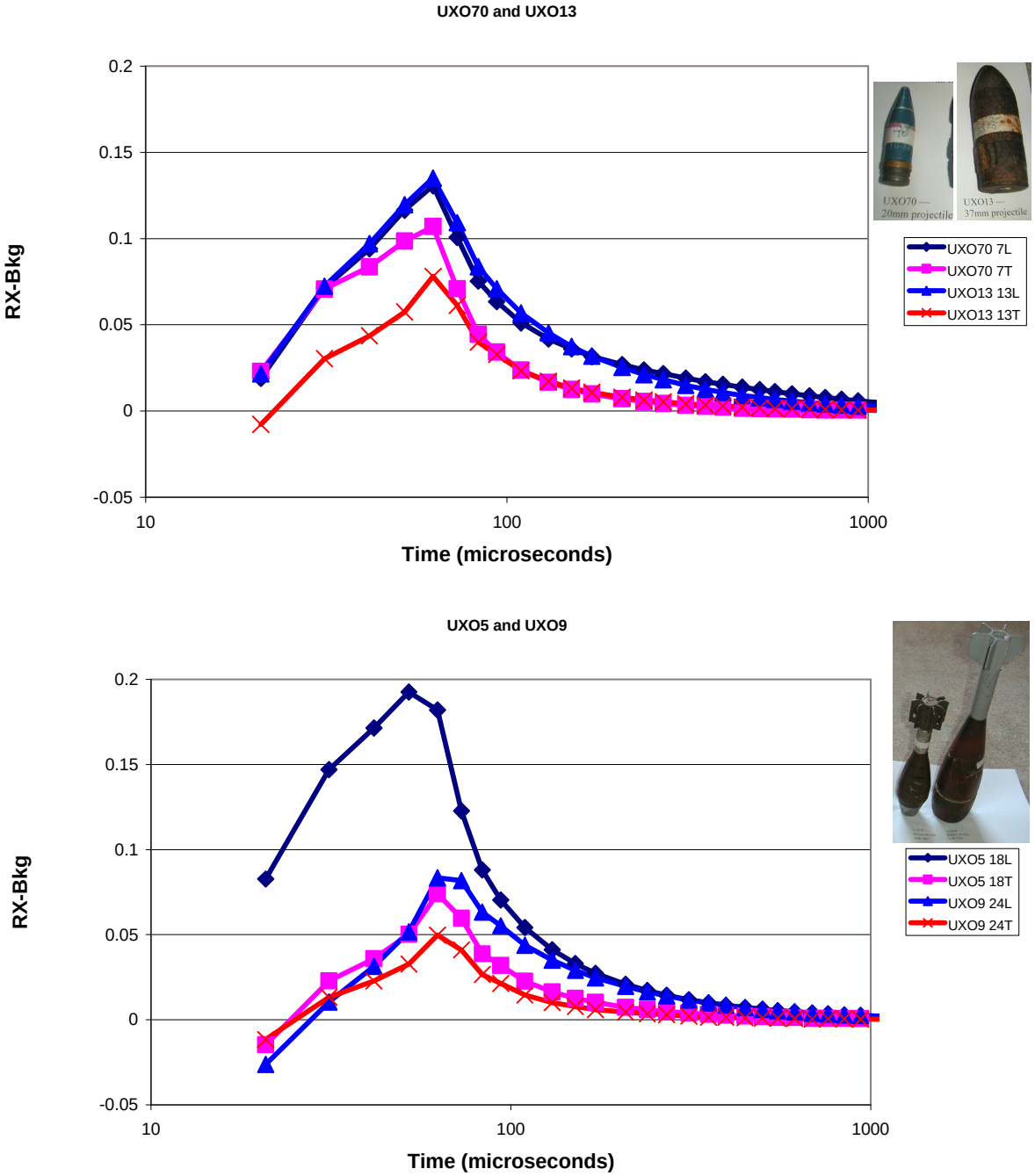

Figure 9. Comparison of the responses of the UXO items #70 and #13 (top), and #6 and #9 (bottom), showing no sign changes during decay. The "T" refers to transverse mode (target oriented long axis perpendicular to sensor coil axis), and "L" the longitudinal mode (target oriented long axis parallel to sensor coil axis). Note the logarithmic time scale, which shows early time behavior.

The results of the matching algorithm for the UXO are summarized in Table 2, showing, for the most part, similar results between the FD and TD data. The scale of the misfits for the two modes is not the same, so direct comparison of misfits between the two modes cannot be made, but the ranking of the target and clutter errors can be compared for each mode. The misfits presented are for the correct library items; in some instances, a better match (lower misfit) was obtained with another item in the library.

	Distance						
Target	[inches]	TD Misfit	FD Misfit				
UXO70	7	0.01	0.01				
UXO70	9	0.02	0.01				
UXO70	15	0.06	0.4				
UXO70	18	0.98	2.33				
UXO12	9	0	0				
UXO12	16	0	0.69				
UXO12	18	0.04	5.6			TD	FD
UXO13	13	0	0.03		Green	8	7
UXO13	22	0.15	0.71		Yellow	8	4
UXO13	26	0.48	4.49		Total	16	11
UXO92	11	0	0		Out of	19	19
UXO92	19	0.04	0.68				
UXO92	21	0.06	4.26				
UXO5	18	0.27	0.01				
UXO5	28	0.46	1.82				
UXO5	32	1.12	2.48				
UXO9	24	0.68	0.01				
UXO9	34	0.89	1.39				
UXO9	39	0.7	4.67				

Table 2. Misfits for responses of UXO items measured at various heights above sensor, matched to their library spectra. Green indicates misfit < .05, yellow < .75; these are arbitrary but chosen merely to visually sort better/poorer fits. Generally, the fitting quality degrades with distance as signal/noise degrades. Overall, performance of the TD mode is comparable to FD, but may be different for some particular targets. Note that these misfits were not always the best from all items in the library – 9 were the best for the FD, while 18 were the best for TD.

The implication of Table 2 is that with the current system and algorithm, the goodness of fit degrades with signal strength and correspondingly target depth, so that in a practical survey, target classification must allow for increasing tolerance with depth.

Table 3 shows the misfits for each library item for the clutter measurements for the FD mode, and Table 4 for the TD mode, with the color highlighting as in Table 1 for visual reference. The TD results indicate a higher rate of “good fits” to clutter, but that is artificial, since the data

scaling, and thus the fitting error, is different between the two modes. A rescaling of the TD when comparing or combining the misfits will be needed to normalize them appropriately.

FD Misfits								
Actual Targets	UXO70_7	UXO12_5	UXO12_9	UXO13_13	UXO92_6	UXO92_11	UXO5_18	UXO9_24
Steel Pipe 14L	0.42	2.81	2.06	0.02	0.4	0.32	0.26	0.04
Steel Pipe 14T	0.98	22.99	26.86	0.06	0.38	0.34	0.06	0.04
Steel Pipe 14D	0.55	9.2	9.32	0.03	0.22	0.19	0.07	0.02
Steel Pipe 20L	1.61	5.79	4.01	0.71	1.5	1.33	1.29	0.47
Steel Pipe 20T	16.45	51.47	48.41	10.29	9.59	9.74	6.94	11.54
Steel Pipe 20D	13.22	31.47	25.93	9.07	9.11	9.07	7.52	9.4
Copper Pipe 10L	2.53	3.59	1.73	1.52	3.29	2.99	3.05	1.06
Copper Pipe 10T	2.25	3.13	1.47	1.39	3.08	2.77	2.88	0.95
Copper Pipe 10D	2.21	3.13	1.5	1.33	3.01	2.71	2.81	0.91
Copper Pipe 17L	11.07	12.67	6.15	8.88	10.88	10.57	10.25	8.14
Copper Pipe 17T	8.27	9.74	4.58	6.48	8.56	8.21	8.1	5.72
Copper Pipe 17D	9.2	10.6	4.99	7.34	9.36	9.02	8.86	6.58
Aluminum Pipe 10L	3.85	6.42	3.98	1.93	4.13	3.88	3.57	1.49
Aluminum Pipe 10T	3.66	5.97	3.61	1.85	4.01	3.75	3.48	1.41
Aluminum Pipe 10D	3.75	6.15	3.72	1.91	4.08	3.82	3.55	1.47
Aluminum Pipe 17L	15.09	18.96	10.62	11.95	13.46	13.28	12.41	11.45
Aluminum Pipe 17T	10.49	14.31	8.01	7.74	9.82	9.56	9	7.08
Aluminum Pipe 17D	11.45	15.13	8.41	8.71	10.54	10.3	9.69	8.1
Screw Driver 7L	1.37	8.43	7.35	0.22	0.93	0.89	0.63	0.15
Screw Driver 7T	1.78	23.98	27.97	0.82	2.51	2.44	0.89	1.37
Screw Driver 7D	1.35	11.39	10.65	0.23	0.86	0.83	0.49	0.21
Screw Driver 14L	3.58	13.94	11.37	1.58	2.49	2.4	2.02	1.34
Screw Driver 14T	55.78	70.91	53.26	45.97	41.76	43.14	35.03	51.02
Screw Driver 14D	11.57	27.14	20.92	7.82	8.24	8.23	7.03	7.86
Nail (10D 3in) 6L	1.82	7.43	5.86	0.48	1.57	1.48	1.18	0.36
Nail (10D 3in) 6T	3.36	9.04	14.8	6.58	6.62	6.83	6.28	7.39
Nail (10D 3in) 6D	1.5	8.14	6.93	0.35	1.24	1.2	0.86	0.31
Nail (10D 3in) 12L	1.93	7.97	6.47	0.53	1.6	1.53	1.19	0.42
Nail (10D 3in) 12T	50.23	58	46.91	42.71	41.24	41.72	35.03	46.49
Nail (10D 3in) 12D	6.61	17.9	13.72	4	5.04	4.9	4.19	3.78
Nut (7/8 in) 5L	0.02	18.23	24.19	0.66	1.23	1.24	0.9	0.82
Nut (7/8 in) 5T	0.21	16.34	19.78	0.17	0.35	0.39	0.19	0.25
Nut (7/8 in) 5D	0.04	17.73	22.82	0.42	0.86	0.87	0.57	0.55
Nut (7/8 in) 10L	6.67	41.66	44.92	2.83	4.06	3.97	1.7	3.61
Nut (7/8 in) 10T	6.51	36.59	37.33	2.95	3.44	3.41	1.85	3.4
Nut (7/8 in) 10D	8.98	44.43	45.34	4.44	5.01	5.01	2.69	5.3
Bolt (3 1/4in) 10L	0.14	1.27	0.9	0.18	0.12	0.09	0.07	0.38
Bolt (3 1/4in) 10T	0.58	21.09	27.52	0.85	2.3	2.24	1.25	1.26
Bolt (3 1/4in) 10D	0.06	3.07	2.81	0.23	0.09	0.07	0.08	0.39
Bolt (3 1/4in) 15L	0.84	3.62	2.33	0.43	0.97	0.81	0.89	0.27
Bolt (3 1/4in) 15T	44.16	84.65	74.44	32.75	29.5	30.67	21.64	38.31
Bolt (3 1/4in) 15D	2.02	8.61	6.77	1.09	1.77	1.61	1.46	0.92
Crushed Coke Can 10T	4.85	20.77	20.48	2.56	3.04	3.14	2.76	2.28
Crushed Coke Can 18T	9.54	30.91	27.62	5.81	5.78	5.83	5.15	5.51
Large Paper Clip 7L	0.22	27.48	38.92	1.09	2.15	2	2.07	0.84
Large Paper Clip 7T	1.15	30.91	46.83	2.33	5.71	5.37	4.45	2.35
Large Paper Clip 7D	0.3	28.54	41.19	1.27	2.83	2.63	2.51	1.05

Table 3. Clutter misfits to library items, measured at several heights/orientations in the FD mode – the number suffix gives the height in inches, and "L", "T, "D" refers to longitudinal, transverse, diagonal orientation. Green indicates misfit < .05, yellow < .75; these are arbitrary but chosen merely to visually sort better/poorer fits. The table is continued on the next page.

FD Misfits continued								
Actual Targets	UXO70_7	UXO12_5	UXO12_9	UXO13_13	UXO92_6	UXO92_11	UXO5_18	UXO9_24
Large Paper Clip 14L	3.81	44.53	54.01	0.9	2.23	1.97	0.66	1.18
Large Paper Clip 14T	6.79	52.99	65.65	2.28	6.05	5.59	2.23	3.39
Large Paper Clip 14D	6.52	49.46	58.42	2.29	4.17	3.84	1.56	3.01
Brass Fitting (1.5in) 5L	3.37	10.16	8.27	1.31	2.88	2.82	2.25	1.16
Brass Fitting (1.5in) 5T	3.34	19.51	20.43	1.72	1.96	2.07	1.8	1.51
Brass Fitting (1.5in) 5D	3.44	13.69	12.24	1.33	2.49	2.5	1.93	1.2
Brass Fitting (1.5in) 10L	4.87	13.59	10.58	2.35	3.99	3.9	3.29	2.06
Brass Fitting (1.5in) 10T	7.22	32.05	30.8	3.93	3.74	3.83	3.29	3.68
Brass Fitting (1.5in) 10D	7.13	23.27	19.71	3.9	4.7	4.7	3.92	3.67
Coat Hanger (twisted) 5T	0.87	17.75	21.35	0.89	1.6	1.75	0.93	1.19
Coat Hanger (twisted) 5L	3.19	16.23	15.96	1.36	2.06	2.13	1.63	1.24
Coat Hanger (twisted) 5D	2.9	16.55	16.64	1.23	1.88	1.96	1.44	1.14
Coat Hanger (twisted) 10T	3.23	26.6	27.94	1.3	2.35	2.4	1.07	1.53
Coat Hanger (twisted) 10L	3.5	18.08	17.68	1.5	2.17	2.22	1.72	1.34
Coat Hanger (twisted) 10D	3.09	18.95	19.16	1.31	1.96	2.03	1.45	1.22
Brass Disk (2"D, 1"H) 9L	0.06	0.79	0.35	0.27	0.2	0.12	0.26	0.38
Brass Disk (2"D, 1"H) 9T	0.73	2.88	1.68	0.3	0.99	0.83	0.89	0.17
Brass Disk (2"D, 1"H) 9D	0.26	1.59	0.82	0.2	0.5	0.37	0.49	0.18
Brass Disk (2"D, 1"H) 16L	5.77	8.93	5.13	4.56	5.55	5.28	5.23	4.11
Brass Disk (2"D, 1"H) 16T	12.67	17.58	10.62	10.14	11	10.81	10.1	9.83
Brass Disk (2"D, 1"H) 16D	6.74	10.88	6.47	5.13	6.22	5.97	5.75	4.69
Bookend 15L	1.72	14.83	15.14	0.47	1.06	1.12	0.63	0.48
Bookend 15T	1.44	13.8	13.91	0.3	0.85	0.9	0.47	0.34
Bookend 15D	1.97	15.2	15.37	0.59	1.13	1.18	0.76	0.54
Bookend 25L	12.96	40.28	35.51	8.23	7.96	8.08	6.3	8.6
Bookend 25T	7.22	28.33	25.24	3.86	4.41	4.44	3.32	3.94
Bookend 25D	6.31	27.9	25.85	3.17	3.59	3.62	2.7	3.14
Paint Can Lid 15V	3.08	25.55	29.42	2.11	1.78	1.86	2.01	1.67
Paint Can Lid 15^	2.84	25.07	29.15	1.99	1.7	1.78	1.92	1.58
Paint Can Lid 15L	0.87	28	35.9	0.78	0.94	0.89	1.05	0.42
Paint Can Lid 25V	4.39	32.54	36.58	2.74	2.24	2.27	2.38	2.23
Paint Can Lid 25^	4.01	31.76	35.45	2.35	1.94	2.04	2.03	1.95
Paint Can Lid 25L	2.66	29.78	34.5	1.46	1.12	1.14	1.28	1.04
UXO Fragment 12T	0.52	16.07	18.46	0.14	0.45	0.52	0.15	0.27
UXO Fragment 12L	1.54	19.82	22.25	0.63	0.88	0.98	0.63	0.59
UXO Fragment 12D	0.71	17.37	19.94	0.22	0.53	0.61	0.23	0.31
UXO Fragment 20T	2.22	22.63	24.18	0.58	1.19	1.14	0.43	0.65
UXO Fragment 20L	3.42	22.95	23.8	1.52	1.84	1.9	1.47	1.34
UXO Fragment 20D	1.22	20.15	22.68	0.24	0.73	0.74	0.23	0.29
Nickel 5	8.4	24.14	44.19	11.74	16.99	16.43	15.96	11.58
Dime 5	19.24	9.42	8.72	20.12	17.03	18.15	15.82	22.55
Penny 5	5.09	14.08	17.03	5.16	4.39	4.72	4.71	5.21
Quarter 5	5	15.41	13.96	2.44	3.79	3.85	3.13	2.26
Quarter 7	12.82	29.14	23.02	8.59	9.23	9.27	8.22	8.27
Quarter 9.5	34.43	57.24	41.99	27.35	24.45	25.15	22.12	28.48
Green FD	3							
Yellow FD	24							
Total	27							
Out of	92							

Table 3 continued. Clutter misfits to library items, measured at several heights/orientations in the FD mode – the number suffix gives the height in inches, and "L", "T, "D" refers to longitudinal, transverse, diagonal orientation. Green indicates misfit < .05, yellow < .75; these are arbitrary but chosen merely to visually sort better/poorer fits.

TD Misfits								
Actual Targets	UXO70_7	UXO12_5	UXO12_9	UXO13_13	UXO92_6	UXO92_11	UXO5_18	UXO9_24
Steel Pipe 14L	0.8	24.77	69.08	0.51	55.47	9.54	3	6.86
Steel Pipe 14T	3.25	36.54	77.68	0.58	39.43	0.89	0.28	2.23
Steel Pipe 14D	1.38	29.58	73.33	0.01	48.17	4.37	0.48	4.67
Steel Pipe 20L	0.8	24.33	69.34	0.73	55.8	10.17	3.41	6.75
Steel Pipe 20T	3.36	36.36	78.26	0.55	39.73	1.14	0.31	2.25
Steel Pipe 20D	1.48	29.96	73.65	0.04	47.78	4.24	0.46	4.61
Copper Pipe 10L	39.29	0.47	0.38	62.94	34.8	0.45	4.85	60.25
Copper Pipe 10T	39.02	0.46	0.32	62.45	35.32	0.41	4.76	60.28
Copper Pipe 10D	39.17	0.47	0.36	62.77	34.98	0.44	4.83	60.24
Copper Pipe 17L	39.29	0.53	0.39	62.92	35.1	0.48	4.88	60.29
Copper Pipe 17T	39.34	0.53	0.39	62.95	35.17	0.46	4.86	60.26
Copper Pipe 17D	39.31	0.52	0.38	63.16	34.92	0.48	4.93	60.15
Aluminum Pipe 10L	41.45	0.71	1.17	66.48	31.07	0.79	5.61	59.93
Aluminum Pipe 10T	41.11	0.66	1.03	66.07	31.51	0.75	5.54	59.93
Aluminum Pipe 10D	41.22	0.69	1.08	66.18	31.44	0.76	5.56	59.94
Aluminum Pipe 17L	41.17	0.74	1.21	67	30.61	0.89	5.85	59.51
Aluminum Pipe 17T	40.92	0.73	1.07	66.43	31.38	0.82	5.71	59.63
Aluminum Pipe 17D	40.85	0.78	1.06	66.34	31.75	0.81	5.69	59.63
Screw Driver 7L	4.21	15.39	41.27	6.02	65.7	5.07	0.35	25.74
Screw Driver 7T	11.71	9.45	21.6	23.14	59.82	1.22	0.57	38.47
Screw Driver 7D	5.03	14.45	38.35	7.97	65.35	4.3	0.15	27.64
Screw Driver 14L	4.29	15.32	40.78	6.36	65.45	4.85	0.39	25.77
Screw Driver 14T	15.8	8.72	17.23	28.93	58.06	1.73	2.27	42.58
Screw Driver 14D	6.42	14.2	35.1	10.3	64.21	3.73	0.36	29.86
Nail (10D 3in) 6L	4.41	15.13	42.26	3.93	68.5	7.32	1.11	26.07
Nail (10D 3in) 6T	18.31	5.73	14.04	26.96	60.87	1.59	0.33	47.32
Nail (10D 3in) 6D	7.01	12.87	35.1	7.74	68.36	5.75	0.49	31.49
Nail (10D 3in) 12L	4.92	14.33	40.98	4.2	69.22	7.36	1.18	27.06
Nail (10D 3in) 12T	17.91	8.8	16.15	28.48	57.01	2.05	1.7	45.67
Nail (10D 3in) 12D	8.51	12.34	32.92	7.93	69.46	6.43	0.88	33.83
Nut (7/8 in) 5L	0.08	26.76	54.73	8.45	49.59	0.61	1.17	12.15
Nut (7/8 in) 5T	3.66	16.8	37.51	14.26	57.52	1.03	0.57	24.58
Nut (7/8 in) 5D	0.99	22.28	47.08	10.96	53.29	0.74	0.9	17.18
Nut (7/8 in) 10L	0.28	25.69	52.75	8.89	50.45	0.61	1.03	13.52
Nut (7/8 in) 10T	4.15	16.27	36.16	14.93	57.65	1.01	0.58	25.62
Nut (7/8 in) 10D	2.31	19.43	41.69	12.78	55.39	0.86	0.72	21.22
Bolt (3 1/4in) 10L	1.6	18.7	52.46	0.84	66.21	9.28	2.22	18.56
Bolt (3 1/4in) 10T	8.23	12.62	27.51	19.6	58.68	1.16	0.63	33.09
Bolt (3 1/4in) 10D	5.07	15.37	38.29	8.6	64	4	0.19	27.69
Bolt (3 1/4in) 15L	56.17	38.52	30.36	29.64	79.12	39.76	31.28	79.1
Bolt (3 1/4in) 15T	86.3	45.05	42.3	52.45	61.46	45.4	39.87	97.19
Bolt (3 1/4in) 15D	73.91	40.87	32.49	41.86	70.51	42.08	35.1	92.29
Crushed Coke Can 10T	59.34	5.77	14.72	67.99	17.79	1.07	4.24	63.85
Crushed Coke Can 18T	59.4	5.67	14.36	67.65	18.26	0.98	4.08	64.29
Large Paper Clip 7L	5.24	15.54	30.67	21.8	54.13	0.26	1.88	27.36
Large Paper Clip 7T	0.33	27	49.01	14.52	46.86	0.31	3.24	13.24
Large Paper Clip 7D	2.82	19.18	37.04	18.82	52.25	0.2	2.17	22.12

Table 4. Clutter misfits to library items, measured at several heights/orientations in the TD mode – the number suffix gives the height in inches, and "L", "T, "D" refers to longitudinal, transverse, diagonal orientation. Green indicates misfit < .05, yellow < .75; these are arbitrary but chosen merely to visually sort better/poorer fits. The table is continued on the next page.

TD Misfits continued								
Actual Targets	UXO70_7	UXO12_5	UXO12_9	UXO13_13	UXO92_6	UXO92_11	UXO5_18	UXO9_24
Large Paper Clip 14L	5.43	15.1	30.37	21.76	54.69	0.28	1.79	27.76
Large Paper Clip 14T	0.3	27.56	49.74	14.18	46.51	0.39	3.25	12.89
Large Paper Clip 14D	3.47	17.94	35.25	19.4	53.18	0.23	1.99	23.69
Brass Fitting (1.5in) 5L	49.61	1.68	4.76	67.73	26.06	0.68	4.7	63.47
Brass Fitting (1.5in) 5T	49.77	1.71	4.85	67.74	25.95	0.68	4.68	63.51
Brass Fitting (1.5in) 5D	62.28	7.12	17.41	65.54	16.8	0.7	3.25	65.34
Brass Fitting (1.5in) 10L	49.61	1.71	4.81	67.75	26.07	0.68	4.71	63.47
Brass Fitting (1.5in) 10T	62.85	7.48	17.96	64.99	16.75	0.65	3.06	65.65
Brass Fitting (1.5in) 10D	53.05	2.78	7.31	67.89	23.9	0.69	4.38	64.31
Coat Hanger (twisted) 5T	10.63	9.81	24.79	18.13	63.38	2.27	0.18	37.4
Coat Hanger (twisted) 5L	5.28	14.58	38.71	7.75	65.72	4.68	0.42	27.65
Coat Hanger (twisted) 5D	6.35	13.5	35.48	9.66	65.62	4.16	0.29	29.96
Coat Hanger (twisted) 10T	10.11	10.12	26.01	16.79	64.03	2.52	0.14	36.62
Coat Hanger (twisted) 10L	5.37	14.49	38.41	7.92	65.69	4.61	0.41	27.84
Coat Hanger (twisted) 10D	6.28	13.62	35.74	9.46	65.63	4.22	0.31	29.79
Brass Disk (2"D, 1"H) 9L	43.58	0.07	0.24	57.16	38.51	0	2.52	65.63
Brass Disk (2"D, 1"H) 9T	45.35	0.31	1	60.92	34.49	0.08	3.22	65.26
Brass Disk (2"D, 1"H) 9D	44.11	0.12	0.42	58.33	37.29	0.01	2.73	65.54
Brass Disk (2"D, 1"H) 16L	44.13	0.13	0.33	57.34	38.55	0.01	2.51	65.94
Brass Disk (2"D, 1"H) 16T	45.92	0.41	1.09	60.65	34.9	0.07	3.09	65.71
Brass Disk (2"D, 1"H) 16D	44.58	0.23	0.55	58.91	37.11	0.03	2.83	65.59
Bookend 15L	6.97	33.43	84.23	2.46	39.04	5.56	1.41	0.78
Bookend 15T	56.74	25.5	62.59	49.25	0.93	2.25	3.01	37.74
Bookend 15D	5.32	32.27	81.46	1.43	42.01	5.36	1.25	1.55
Bookend 25L	6.64	33.16	83	2.52	40.45	6.19	1.78	1.19
Bookend 25T	56.04	24.77	61.54	50.72	1.1	2.63	3.49	37.26
Bookend 25D	11.36	35.23	88.29	5.56	32.96	5.8	1.91	0.31
Paint Can Lid 15V	61.73	29.62	67.72	43.81	1.3	2.03	2.44	38.87
Paint Can Lid 15^	65.37	27.51	61.85	46.5	1.6	1.52	2.1	44.67
Paint Can Lid 15L	60.49	31.87	71.88	40.2	1.17	1.82	1.98	36.41
Paint Can Lid 25V	65.14	24.85	57.65	50.42	2.16	1.96	2.84	45.93
Paint Can Lid 25^	62.53	31.53	70.04	40.82	1.07	1.56	1.77	39.03
Paint Can Lid 25L	64.44	26.39	61.1	47.98	1.7	1.95	2.57	43.91
UXO Fragment 12T	56.75	31.61	72.32	39.69	0.59	1.31	1.37	34.62
UXO Fragment 12L	3.58	16.82	42.08	8.22	62.02	3.26	0.28	23.87
UXO Fragment 12D	61.74	29.61	65.99	42.91	0.66	0.89	1.13	41.53
UXO Fragment 20T	60.66	29.06	66.06	43.55	0.6	1.01	1.36	40.61
UXO Fragment 20L	1.83	19.91	50.63	4.42	60.54	4.07	0.41	18.2
UXO Fragment 20D	52.82	33.66	77.49	36.1	1.29	1.64	1.41	29.41
Nickel 5	79.74	67.35	81.07	10.32	9.59	13.84	12.84	52.92
Dime 5	64.99	9.49	22.3	64.54	14.29	1.04	3.33	64.39
Penny 5	76.26	22.29	42.94	48.4	8.4	0.59	0.81	65.09
Quarter 5	52.54	3.16	8.36	70.61	21.65	1.38	5.6	61.8
Quarter 7	52.44	3.12	8.44	70.88	21.32	1.45	5.75	61.54
Quarter 9.5	53.11	3.2	8.89	70.66	20.91	1.49	5.64	61.86
Green TD	6							
Yellow TD	61							
Total	67							
Out of	92							

Table 4 continued. Clutter misfits to library items, measured at several heights/orientations in the TD mode – the number suffix gives the height in inches, and "L", "T, "D" refers to longitudinal, transverse, diagonal orientation. Green indicates misfit < .05, yellow < .75; these are arbitrary but chosen merely to visually sort better/poorer fits.

Although a number of the clutter items generate a response that matches a UXO item in the library, there are a significant number that do not. The ability to reject clutter may improve if the TD and FD data were fused; a first attempt using a simple sum (or average) of the two mode misfits only gave slight improvement; a more sophisticated method, or even an optimally weighted misfit, may further improve results.

Conclusions

A single EMI instrument can operate as either a time domain or frequency domain sensor, and provide both simultaneously by alternating between them. Simple target classification algorithms developed for the FD mode can be adapted to the TD mode obtaining similar performance. Combining FD and TD data has potential to improve clutter discrimination performance, but it is not achieved with a simple sum.

We have successfully modified and tested a GEM-3 to operate in a dual mode in which FD and TD data are obtained over alternating 30 Hz intervals. We have developed prototype firmware for the GEM that allows programmable transmitter current on/off durations and measurement time gating. Preliminary testing has included survey operation on a moving platform over a seeded test bed, and controlled in-air experiments for UXO and clutter discrimination and identification.

To fully realize the optimal performance, more work on data processing (TD particularly) and FD/TD fusion is required. Also, some hardware optimizations for dual mode could be evaluated; the hardware as designed is functional, but some fine-tuning with dual mode in mind may be possible.

Future Work

Detection

We have demonstrated that the GEM-3 time domain data detects buried metallic objects consistent with the frequency domain data in our small-scale Geophex test bed. The current algorithm – a simple summation over multiple time gates – is the only scheme tested so far, so there is potential to further optimize the detection channel. Candidates could be as simple as unequal weighting of the channels in the summation (i.e. weighting later times more heavily may reduce the response to geology and small surficial metal fragments), or as complex as apparent conductivity algorithms.

The goal is to enhance the standard frequency-domain performance of the GEM-3, and we hope to extract some characteristics in the time-domain response that is either more sensitive to some targets of interest or less sensitive to certain sources of noise (including geology or clutter). If the frequency domain has some advantages for some targets and/or environments while the time domain has advantages for others, then a dual-mode system will have overall advantage over either by itself. Combining the detection channels for the two modes needs to be done, and finding an algorithm that exploits the advantages of each is desired. We have not yet fully

explored this issue, and need to perform more extensive testing of various combinations of detection schemes in standard and dual modes.

Discrimination

The time-domain response has been shown to provide target identification capability, with clutter discrimination based on poor fits to known target responses. The fitting algorithm tested thus far uses a simple squared error sum over all time gates, and there is potential for improvement. Analogous to the detection algorithms, simple improvements may be unequal weighting of the errors or different time gates, and more complex algorithms might entail parameterizing the response as a sum of decay functions (such as decaying exponentials or an Oldenburg model of inverse power – decaying exponential products). The model parameters can then be used to match a library of known UXO, or they can be used to classify targets (i.e. aspect ratio and symmetry).

Overall enhancement of the GEM-3 discrimination capability will be realized if, for at least some UXO or some clutter, the classifying is more robust using dual-mode data than when using only frequency domain data. An optimum way to mix the results must be developed (we have simply averaged the misfits so far), which may entail linear but unequal weighting or a more complex non-linear function.

Proposed Tasks

A two-year program would allow us to achieve the full potential of the dual-mode GEM-3. In addition to the data processing effort described above, we will look into possibly increasing the current capacity to increase the magnetic moment of the TX coil as well as other hardware modifications that might improve the TD performance without degrading the FD performance.

Our major effort will be devoted to developing algorithms for UXO detection and discrimination using the *combined dual-mode data* from the FD and TD operation. Once completed, we will evaluate the FD-TD GEM-3 initially at the Geophex UXO Test Site in Raleigh, NC, and determine its usefulness, particularly for deeply buried targets. The site contains 21 metal pipes and a magnetic rock in a 10m by 10m plot. After we complete our in-house testing, we will perform a formal demonstration at on of the ESTCP UXO test sites.

We have completed the seed project, and propose a follow-up development program, including:

- Investigate and implement increasing the TX moment,
- Develop a combined FD-TD detection software,
- Develop more sophisticated combined FD-TD discrimination software,
- Evaluate the detection/discrimination capability at the Geophex UXO Test Site,
- Demonstrate the new FD-TD sensor at ESTCP demo sites.